Morphological Characterization and Modelling of Electrical Conductivity of Multi-Walled Carbon Nanotube / Poly(p-Phenylene Sulfide) Nanocomposites Obtained by Twin Screw Extrusion

A. Noll, T. Burkhart

Morphological Characterization and Modelling of Electrical Conductivity of Multi-Walled Carbon Nanotube / Poly(p-Phenylene Sulfide) Nanocomposites Obtained by Twin Screw Extrusion

A. Noll, T. Burkhart

PII: S0266-3538(10)00494-X
DOI: 10.1016/j.compscitech.2010.12.026
Reference: CSTE 4891

To appear in: *Composites Science and Technology*

Received Date: 22 July 2010
Revised Date: 14 December 2010
Accepted Date: 18 December 2010

Please cite this article as: Noll, A., Burkhart, T., Morphological Characterization and Modelling of Electrical Conductivity of Multi-Walled Carbon Nanotube / Poly(p-Phenylene Sulfide) Nanocomposites Obtained by Twin Screw Extrusion, *Composites Science and Technology* (2011), doi: 10.1016/j.compscitech.2010.12.026

Morphological Characterization and Modelling of Electrical Conductivity of Multi-Walled Carbon Nanotube / Poly(p-Phenylene Sulfide) Nanocomposites Obtained by Twin Screw Extrusion

A. Noll[a*], T. Burkhart[b]

[a] *Institute of Composite Materials GmbH, Materials Science, Erwin Schroedinger Str. 58, 67663, Kaiserslautern, Germany*

** corresponding author. Tel.: +49 631 2017 435. Fax: +49 631 2017 196. E-mail address: andreas.noll@ivw.uni-kl.de*

[b] *Institute of Composite Materials GmbH, Materials Science, Erwin Schroedinger Str. 58, 67663, Kaiserslautern, Germany*

A B S T R A C T

In this study, poly(p-phenylene sulfide) based nanocomposites containing multi-walled carbon nanotubes (MWNTs) were produced by dilution of a 15 wt.% MWNT/PPS masterbatch via twin screw extrusion process. The electrical conductivities of the nanocomposites were measured and percolation threshold was observed below 0.77 vol.% MWNTs. The state of dispersion and distribution quality of MWNTs was analyzed on macro- and nanoscale through transmission light and scanning electron microscopy (SEM). A good deagglomeration of primary macroagglomerates and a homogenous MWNT distribution on nanoscale was found. The dependence of conductivity on MWNT concentration was estimated using statistical percolation theory which matches the experimental data quite well. A new empirical equation was set up to fit the electrical conductivity using quantitative values of visible percolating MWNTs which were detected by charge contrast imaging in SEM.

Keywords:

A. Nano composites

A. Carbon nanotubes

B. Electrical properties

C. Modelling

D. Scanning electron microscopy (SEM)

1 Introduction

The modification of electrically isolating polymer matrices with carbon nanotubes (CNTs) is of great interest in both academic and industrial research. CNTs exhibit outstanding mechanical performance, high electrical and thermal conductivity as well as chemical stability, thus making them promising fillers in multifunctional polymer nanocomposites [1-3]. One of the promising applications of CNTs is to achieve electrical conductivity in polymers using very low filler contents without loosing other inherent properties of the polymer matrix. Conductive polymer composites based on CNTs offer many interesting applications in the manufacture of sensors, microelectrodes, electromagnetic shielding materials etc. [4]. The variation of many parameters of CNT nanocomposites like CNT type, synthesis method, treatment and dimensionality as well as polymer grade will make a detailed understanding of applied processes difficult [5]. Basically, an increase of conductive filler concentration usually results in a transition from a non-conducting to a conducting state at a threshold concentration. Thereby, conductive fillers built a percolated network throughout the polymer matrix with a filler concentration higher than percolation threshold. CNTs own a high aspect ratio (100-1000) and a high specific surface, whereby, very low percolation threshold concentration can be realized. A review of experimental and theoretical work on electrical percolation of CNTs in polymer composites is given by Bauhofer et al. [5]. A review of 488 papers on the subject of CNT polymer composites [6], published in 2010, clearly reveals a large variation of the electrical properties values as a function of polymer matrix, processing method and CNT type.

The commonly used methods to produce thermoplastic CNT nanocomposites are in-situ polymerization, solution route, and melt compounding [7-9]. Melt processing is the preferred method for large scale compounding of thermoplastics [10], as it is based on conventional technologies like twin-screw extrusion and injection molding. In recent years, the interest of industry is increasing drastically to use MWNTs in standardized manufacturing processes as

reinforcing or functional fillers, in particular due to large-scale production and falling prices of MWNTs. Masterbatch dilution method or direct compounding can be performed. It is always a challenge to realize a well deagglomeration of primary CNT-bundles and building up a well defined interface and CNT dispersion [8,11]. The path of a masterbatch dilution by twin-screw extrusion is a common used and appropriate method to produce CNT nanocomposites [10,12,13]. CNTs are strongly effected by van der Waal`s attraction just to their small size and therewith high surface area, and besides they are strongly physically entangled, which is a major challenge for process control to disperse the primary CNT agglomerates [14]. The overall development chain from compounding to further processing like hot pressing or injection molding have to be considered, due to their significant influence on deagglomeration and distribution state [15,16], orientation, and possible secondary agglomeration of CNTs depending on processing parameters and methods [10,15,16]. This entire value chain can completely change the properties, especially the mechanical and electrical properties, and therefore must be considered.

To built up structure property relations, the resultant CNT dispersion and network formation, can be analyzed on nanoscale using charge contrast imaging in scanning electron microscopy, as an alternative to transmission electron microscopy [17-19].

PPS is a semi-crystalline aromatic polymer with outstanding high-temperature stability, inherent flame retardancy, good chemical resistance and excellent friction properties, widely applied in commercial and industrial fields for example automotive and aerospace engineering [20-22]. However, the applications of neat PPS have been somewhat limited due to relatively low glass transition temperature (~ 90°C) compared to its high melting temperature (~ 275°C) and its tendency towards brittleness. Therefore, PPS is mostly reinforced with short glass fibers, carbon fibers or other reinforcing fillers to overcome these disadvantages. Hitherto many micro- or nano-fillers such as short glass fiber, silicon dioxide, expanded graphite,

metal and its oxide/sulfide have been successfully compounded with PPS. Majority of those works focused on the tribological and mechanical properties, crystallization and conductivity behavior [23]. The addition of nanofillers like CNTs is another interesting possibility to optimize the mechanical and electrical performance profile of PPS. Up to now, there exist a limited number of works concerning high temperature thermoplastic polymers modified with CNTs, especially poly(p-phenylene sulfide) (PPS) as polymer matrix. Han et al. [24] found a electrical percolation threshold at 3 wt.% of MWNTs in PPS after direct melt compounding and injection molding. Yu et al. [7] founds these threshold value between 1 and 2 wt.%, and a higher percolation threshold of 5 wt.% was shown by Yang et al. [22], using melt compounding and hot pressing for compounding and specimen preparation, respectively.

The goal of this work was to analyze the electrical conductivity and determine the percolation threshold of multi-walled carbon nanotubes (MWNT)/PPS nanocomposites, produced via twin screw extrusion and injection molding, considering the entire value chain using commercial available PPS and MWNTs. The formation of MWNT network structures as well as the degree of deagglomerated MWNT bundles was studied by using transmission light and scanning electron microscopy (SEM). Moreover, the conductivity of MWNT/PPS nanocomposites was described by using the statistical percolation theory [25], which predicts the conductivity as a function of filler concentration. Furthermore, an empirical power law equation, similar to statistical percolation theory, was found to fit the electrical conductivity of MWNT/PPS-nanocomposites by using quantitative values of percolated MWNTs on nanoscale, which were determined by using quantitative analysis of charge contrast SEM images.

2 Materials

Granular linear poly(p-phenylene sulfide) (PPS) were provided by Ticona GmbH, Germany (Fortron 0205P4). The used multi-walled CNTs (MWNT) were supplied by Bayer Materials

Science AG, Germany (Baytubes® C150P), with an outer diameter of ~ 13 nm, an inner diameter of ~ 4 nm, and a length of a few micron [17,26] (Fig. 1). A 15 wt.% MWNT/PPS masterbatch was produced by Ensinger GmbH, Germany, by twin screw extrusion.

Systematic dilutions of the masterbatch (1, 2, 3, 4, 5 wt.%) in PPS matrix was performed on pilot line scale via co-rotating twin screw extruder (ZE25x44, Berstorff GmbH, Germany). The 15 wt.% masterbatch was extruded a second time with same extrusion parameters than the dilution step. Therefore, definite amounts of dried virgin PPS and masterbatch granulate were fed via gravimetric high-precision feeder (K-tron GmbH, Germany) through the main hopper into the barrel of the machine, whereby defined MWNT concentrations in nanocomposites were realized. The applied processing parameters are temperature of the barrel (T = 310°C), throughput (9 kg/h), and screw rotation speed (300 rpm). This is a continuous production process with a residence time of about one minute [27]. The extrusion screw was modular assembled with conveying elements, kneading elements and back conveying elements, to introduce high shear forces for MWNT deagglomeration. It is shown in [27] that such a screw setup is practicable for deagglomeration of spherical ceramic nanoparticle agglomerates, which was used in this study for MWNTs dispersion and distribution. The possible screw configurations and screw elements are described in [16].

After compounding, the granulated compounds were dried for 4 hours at 120°C and manufactured to tensile bars and plates via injection molding (Allrounder 320S, Arburg GmbH, Germany). The injection molding parameters have a significant influence on resulting materials properties, especially on CNT network formation and orientation [28,29]. Low injection speed and high melting temperature seemed to be favorable to obtain good electrical conductivity [29]. The injection molding parameters was kept constant for all MWT/PPS-nanocomposites. The main parameters are injection speed of 41.5 mm^3/s, melting temperature of 320°C, mold temperature of 145°C and cooling time of 25 s.

3 Experimental details

3.1 Measurement of electrical conductivity

High resistant compounds with a electrical conductivity less than 10^{-4} S/m were measured according to DIN IEC 60093 (VDE 0303 Part 30, 1993), using a electrometer (6517A, Keithley Instruments GmbH, Germany) connected with a ring electrode test fixture (8009 Resistivity Test Fixture, Keithley Instruments GmbH, Germany). Therefore the injection molded plates with a thickness of 3 mm, a length of 87 mm and a width of 80 mm were used.

The specimen with an electrical conductivity $>10^{-4}$ S/m were determined according to DIN EN ISO 3915 (1999). A four-point test fixture, two electrodes for power supply and two electrodes for measuring the potential difference, combined with a Keithley 2601A electrometer was used. The specimens were cut out of injection molded tensile bars with a length of 60 mm (injection molding direction), a thickness of 4 mm, and a width of 10 mm. The measurement direction was equal to the injection molding direction. For optimum contact between composite and electrodes, the surfaces to be conducted were coated with silver paste. The entire bulk material is therewith contacted and can contribute to the current flow due to the overall contact of the cut surfaces. At least four samples of every nanocomposite were measured for statistical validation. The electrical conductivity could be determined by the following equation:

$$\sigma = I/\Delta U * L/A \qquad (1)$$

Where I is the current flow, ΔU is the potential difference between the two measuring electrodes, A is the surface perpendicular to the current flow direction, and L is the distance between the measuring electrodes.

3.2 Microscopy

The fraction of remaining primary macroagglomerates of MWNTs in PPS was investigated by transmission light microscopy. Thin sections with a thickness of 4 µm were cut from injection

molded specimens containing 1, 2 and 4 wt.% of MWNTs using a microtome (HM355S, Microm GmbH, Germany). These slices were fixed on glass plates for transmission light microscopy, observed with a magnification of 40 x (Digiplan Leitz GmbH, & Co. KG, Germany). The microscope is combined with a digital camera (A4i DIG 3300, Olympus GmbH, Germany) to record the images. These images were software analyzed (analySYS FIVE, Olympus GmbH, Germany) to determine the fraction of agglomerates in the respective section. The phase fraction A/A_0 is the area A of agglomerates with a median agglomerate diameter > 2 µm in correlation to the total observed area A_0 in %, whereby a dispersion index D of MWNTs can be calculated by the following equation, which was also used by Krause et al. [4] and Villmow et al. [12]:

$$D = (1-f*(A/A_0/\Phi_{MWNT}))*100\% \quad (2)$$

Wherein *f is* the factor describing the effective volume of the filler in agglomerate and was set to 0.25 for MWNTs, which was also used in [4] and [12], and Φ_{MWNT} is the volume fraction of MWNTs. The dispersion quality of the masterbatch couldn't be observed due to its light resistance because of high MWNT load.

High resolution images were taken using a field emission scanning electron microscope (FESEM) (Supra™ 40 VP, Carl Zeiss SMT AG, Germany) to analyze the MWNT network in PPS on nanoscale. Therefore, surfaces of cryo-fractured samples parallel to injection molding direction were detected without any additional conductive coating, to perform a contrast imaging between percolated MWNTs, isolated MWNTs and the electrical isolating PPS-matrix. The images were taken from the core zones of injection molded samples. A low acceleration voltage of 0.5 kV, a working distance of about 4-5 mm and an in-lens detector were used to observe the MWNTs network in high quality, and with an improved contrast between the percolating MWNTs and the matrix. This contrast mechanism (Charge Contrast Imaging (CCI)) was described by Chung et al. [30] and was already applied by different

working groups [17-19,31]. Commonly acceleration voltages ≥ 10 kV were used to obtain an optimized contrast and depth information in charge contrast imaging. In this study 0.5 kV leads to the best contrast. The best operation parameters are probably dependent on polymer matrix, functional filler and filler matrix interaction. The used low acceleration voltage of 0.5 kV leads to low depth information, and therewith only near surface information of MWNT structure.

Fig. 2 shows the charge contrast principle, visualizing only the percolated conductive fillers (in our case the MWNTs), by having a higher potential to emit secondary electrons than the surrounding dielectric area. This outlines the huge potential of charge contrast imaging to investigate the real percolated nanotube structure, without the need of transmission electron microscope (TEM). Furthermore, the contrast difference between the percolated MWNTs and surrounding area was high enough for quantitative phase analysis of percolating MWNTs. This analysis was performed in the same way like the light microscopy analysis of macroagglomerates using analyzing software (analySYS Five, Olympus GmbH, Germany). With this powerful technique, a new value, the so called CCI-factor (A_{MWNT}/A_o) can be determined, which is the quantitative phase amount of percolating MWNTs (A_{MWNT}) in the charge contrast images to the overall picture area (A_0). A_{MWNT} was determined using only the bright MWNTs in CCI-images by manual phase separation of histogram peak. From each nanocomposite 10 CCI-images were analyzed, the mean phase amount and standard deviation were determined. Depth information due to surface roughness or penetration depth of the electron beam can not be given by these investigations. Assuming all composites have a similar topology and penetration depth of electron beam, we get a very well impression of percolate MWNT structure more or less in two dimensions depending on MWNT load.

With these two microscopic techniques a quantitative analysis of the MWNTs on macro- and nanoscale is possible, and structure property relationships can be set up.

4 Prediction of electrical properties of composites

4.1 Percolation theory (scaling law)

In 1957, Broadbent and Hammersley [32] introduced the term "percolation theory" and used a geometrical and statistical approach to solve the problem of fluid flow through a static random medium. The concept of percolation has been applied to many diverse applications. One class of those materials is constituted of mixtures of electrical conducting and insulating matrices. The main question concerning these mixtures is how the conductivity changes with content of the conductive filler. To understand the network formation on scientific level, many so-called percolation models and equations have been discussed in literature, and are reviewed by Lux [33]. The percolation theory has been used to interpret the behavior in a mixture of conducting and nonconductive components above the percolation threshold [34]. The sudden transition in such materials from insulator to conductor is evidence of a percolation threshold. A simple power law describes the relation between composite conductivity and conductive filler concentration in the vicinity of the percolation threshold and is frequently applied for CNT polymer composites [17,35-38]:

$$\sigma_c = \sigma_0 (\Phi_f - \Phi_c)^t \quad (3)$$

where σ_c is the composite conductivity, σ_0 is the conductivity of conductive reinforcement or saturation conductivity, Φ_f is the volume fraction of reinforcement, Φ_c is the percolation threshold and t is the critical exponent. The volume contents of MWNTs were calculated using materials densities of 1,39 g/cm^3 for PPS and 1,75 g/cm^3 for MWNTs [39]. This equation is valid at concentrations above the percolation threshold. The value of the critical exponent t is dependent on two or three dimensional lattice of percolating network. Quite often, experimental results are fitted by plotting $\log(\sigma_c)$ vs. $\log(\Phi_f - \Phi_c)$ as a function of variation of the percolation threshold filler content until the best linear fit is obtained. In case of t between 1.5 and 2, there will be a good match with the calculated values for a three-dimensional system. As shown in the review of Bauhofer [5], the yield values of t of CNT

nanocomposites is predominantly in the range from 1.3 to 4, peaking around $t = 2$. Foygel et. al [40] shows for homogeneous randomly distributed and oriented spherocylinders in a 3D system, that the critical exponent decrease significantly ($t < 1.6$, which indicates theoretically a 2D network), with increasing aspect ratio ($> 10^2$).

5 Results and discussion

5.1 Morphology

Transmission light microscopy and SEM were carried out to study the distribution, dispersion and structure of incorporated MWNTs on macro- and nanoscale to set up structure property relations. These images were software analyzed to get quantitative results of macroagglomerate fraction and fraction of percolated individual MWNTs on nanoscale.

Fig. 3 shows the phase fraction of macroagglomerates (remaining agglomerates) for samples containing 1, 2 and 4 wt.% MWNTs, analyzed via transmission light microscopy. The phase fraction of macroagglomerates increases from 0.53 % for 1 wt.% MWNTs to 1.1 % for 4 wt.% MWNTs. The calculated dispersion index *D* increases form 83 % for 1 wt.% MWNTs to 91 % for 4 wt.% MWNTs. Thus, a sufficient good deagglomeration of primary agglomerates can be observed. Furthermore, a better dispersion quality (higher dispersion index) was achieved at higher MWNT contents. Villmow [12] got comparable dispersion indices with optimized process parameter of the twin screw extrusion for MWNT in poly(lactic acid) matrix.

The nanostructure was observed using charge contrast imaging (CCI) in the field emission scanning electron microscope (FESEM). Fig. 4 (a) and b)) compares the topography and CCI images of the same sample position of nanocomposite containing 2 wt.% MWNTs, which were recorded at the same time. The MWNTs couldn't be observed in topography image. Quantitative topographic data such as surface roughness can not be gained from these SEM images. Fig. 4 a) reveals the assumed good impregnation of MWNT agglomerates. The

erosion as dispersion process is seen in Fig 4 b). The two dispersion mechanisms rupture and erosion are described in [14]. The CCI, however, exhibit clearly the MWNT backbone structure at the surface (Fig 4 c)). The nanotubes are homogenously dispersed in the matrix and individual MWNTs can be clearly detected. They appear curved, wrapped and partially tangled. These images are the proof of principle that percolation will be built up via nanodispersed MWNTs providing the charge contrast and not via percolated macroagglomerates. This underlines that the charge contrast SEM imaging (CCI) is a powerful tool to visualize the distribution of MWNTs in polymer composites even on several length scale. Fig. 5 shows charge contrast images of 2 wt.% (a), 3 wt.% (b), 4 wt.% (c) and 5 wt.% (d) MWNT nanocomposites and the gray scale histogram, respectively. In all cases, a homogeneous nanodistribution of MWNTs can be observed. A secondary agglomeration of MWNTs in the core zone of injection molding specimen, as they have been recognized on hot pressed MWNT/PC composites [10,15] or online measurement of electrical conductivity during rheological tests [41,42] could not be observed. Kasaliwal et al. [15] have shown that secondary agglomeration and therewith a significant improvement of electrical conductivity near percolation threshold of MWNT/PC nanocomposites was observed, due to secondary agglomeration. Such a secondary agglomeration is caused by long processing times (> 1 min) and low shear rates during long term melt mixing [10,15], and depends amongst others on matrix viscosity, CNT type and CNT/matrix interaction. Such a secondary agglomeration is not expected in our case due to the short processing time and cooling time of 25 s in injection molding process, which is confirmed by CCI images. The recognized short pull out length (< 1µm) of MWNTs is an indication for good interfacial adhesion which can be explained via π-π electron stacking, interchanges respectively between tubes and the PPS polymer containing aromatic ring structures [22], even though the MWNT surfaces are not functionalized. Furthermore, this interaction of PPS and MWNTs leads to good impregnation of primary agglomerates after incorporation of MWNTs in PPS melt during melt mixing (Fig. 4 a)),

whereby the shear forces are introduced into the agglomerate, which results in a good deagglomeration of primary MWNT-bundles. Up to now, no method is known, which allows accurate determination of final MWNT length in the matrix after processing. By using CCI-images, comparative studies can be set up but an exact length distribution can not be determined. The histogram width of the evaluated bright CNTs in charge contrast imaging is in the range of 80 up to 130 nm (Fig. 8), which was kept constant for all images by the operator, adjusting brightness and contrast. The observed thickness is about five to ten times lager than actual thickness of MWNTs (~ 13 nm), which is due to edge blurring at MWNTs or potential of interphase between PPS matrix and MWNTs to emit electrons and is not yet fully understood. However, the respective phase fractions of percolated MWNTs, and therewith visible MWNTs, increase with increasing MWNT content, and the calculated CCI-factor can be used for empirical fit of electrical conductivity of MWNT/PPS-nanocomposites.

5.2 Percolation threshold and modelling of electrical conductivity

Fig. 7 depicts the conductivity of nanocomposites in injection molding direction as a function of MWNTs load in vol.%. The volume fraction was calculated by using materials densities (1,39 g/cm^3 for PPS and 1,75 g/cm^3 for MWNTs [39]). The percolation threshold was found lower than 0.77 vol.% (1 wt.%). The conductivity changes of 14 decades between unfilled PPS and 1 wt.% MWNT concentration. A further increase of MWNT loading (> 1 wt.%) leads to a moderate increase of conductivity. 15 wt.% MWNT nanocomposite has the highest conductivity with 54 S/m.

Inset in Fig. 7 illustrates a linear regression fit of the specific conductivity as a function of (Φ_{MWNT}-Φ_C) by the log-log plot too. According to equation 3, a percolation threshold of 0.3 vol.%, a saturation conductivity, σ_0 of 4025 S/m, and scaling exponent t is 1.9 were determined. There is a good quantitative correlation between the experimental data and the power law theory (99.1%). The critical exponent matches very well with predictions from

statistical percolation theory for a three-dimensional conducting network in an isolating matrix [5,25]. Kovacs et al. [43] observed the existence of two types of percolation thresholds, which is a characteristic feature of composite materials, passing a fluid state of low viscosity during processing. The higher threshold is determined by statistical percolation theory. The lower one can vastly be shifted down to lower concentrations by stimulating particle flocculation and network formation. In that case a new simple geometrical model was introduced. Such an assumption is in our case not necessary due to a homogenous CNT dispersion. Various working groups built up new methods to find relationships between processing, structure, and properties of CNT composites, e.g. on applying spatial statistics to TEM images on nanoscale [44], correlate deagglomeration states on microscale with electrical properties [14], or built up relationships by means of indirect measuring methods such as DSC [45] or rheological studies [42,46].

In this paper we introduce a new empirical fit using equation 4, whereby the conductivity of the MWNT nanocomposites can be taken from the measurable CCI-factor, the phase fraction of percolating CNTs (A_{MWNT}/A_0) in charge contrast SEM images. In these studies, the brightness of MWNTs in CCI images was kept constant by the operator, and the operator adjusted the threshold of histogram peak to distinguish the phase amount of bright MWNTs in similar appearance. Afterwards, a quantitative analysis was carried out.

The following empirical equation was set up, to correlate the electrical conductivity with phase amount of bright MWNTs in CCI images.

$$\sigma_c = \sigma_0 (a*CCI\text{-}Factor)^b \quad (4)$$

Where σ_c is the composite conductivity, σ_0 is the conductivity of conductive reinforcement or saturation conductivity, a is a correction factor reg. surface topography and b is the exponent. The higher the surface area the lower should be the value a. Fig. 8 shows the log-log plot of σ_c vs. the phase fraction of percolated MWNTs (CCI) determined by quantitative analysis of

CCI multiplied by the correction factor *a*. This empirical fit matches the experimental data of electrical conductivity of MWNT/PPS nanocomposites quite well (99.1%).

The correction factor *a* was set to 0.1 and 1 to show its influence on saturation conductivity. σ_0 is 385 S/m for $a = 0.1$ and $3*10^5$ for $a = 1$. In case of the saturation conductivity of 4025 S/m, based on the general percolation theory, we obtain a value for the fit parameter *a* of 0.466, which is in a good agreement to the surface topography. The exponent b = 2.9 can not be correlated with the critical exponent *t* of the percolation theory, and it is up to know not possible to give any dimensional information. In further studies the correction factor *a* should be quantified in a more detailed way especially via analyzing the surface topography as a function of variation of matrix material, CNTs type and processing parameters. However, this new technique and empirical approach offer the possibility to apply the power law model with a measurable variable (CCI-factor).

6 Conclusion

The MWNT/PPS nanocomposites, produced via a two step twin screw extrusion process, show a sufficient dispersion sate of primary macroagglomerates to be detected with software analyzed transmission light microscopy images. An electrical percolation threshold is obtained at about < 0.77 vol.% (1 wt.%). The conductivity has been explained in terms of percolation theory. The observed critical exponent of electrical conductivity, $t = 1.9$, is the near the universal value (t = 2) for random 3D percolation network. A homogeneous distribution state of MWNTs on nanoscale could be detected using charge contrast imaging in FESEM. Therewith, a quantitative value of percolated MWNTs on nanoscale (CCI-Factor) was determined. This value could be linked with a power law equation which is a new empirical approach to estimate electrical conductivity of MWNT nanocomposites with MWNT contents higher than percolation threshold.

Acknowledgement

The authors thank the Bundesministerium für Bildung und Forschung (BMBF) for financial support within the project 03X0042J, and Ticona GmbH for providing the poly(p-phenylene sufide) (Fortron 0205P4).

Figure captions

Fig. 1 SEM image of primary MWNT agglomerates (Baytubes® C150P).

Fig. 2 Principle of Charge Contrast Imaging (CCI) by SEM.

Fig. 3 Phase fraction of macroagglomerates (> 2 µm) for MWNT/PPS nanocomposites with 1 wt.%, 2 wt.% and 4 wt.% MWNT and the corresponding dispersion index *D*.

Fig 4. Secondary electron SEM images of an unsputtered surface of a nanocomposite containing 2 wt.% MWNT near an agglomerate: topography (a), CCI image of percolated MWNTs (b) and CCI image of homogeneous distributed MWNTs.

Fig 5. CCI-SEM images of different MWNT concentrations in PPS: 2 wt.%, (a) 3 wt.% (b), 4 wt.% (c); 5 wt.% (d).

Fig 6. CCI-SEM images of different MWNT concentrations in PPS: 2 wt.% and 4 wt.% pf MWNTs and the histrogramm width of bright CNTs. Respectively.

Fig 7. Electrical conductivity of PPS-based nanocomposites as a function of volume fraction of MWNT. Inset: A log-log plot of the electrical conductivity of PPS based MWNT nanocomposites as a function of (Φ_{MWNT}-Φ_C) with the fit line according to equation 3.

Fig 8. A log-log plot of the electrical conductivity of PPS based MWNT nanocomposites as a function of (a*CCI-Factor) with the fit line according to equation 4.

References

[1] Chang TE, Jensen LR, Kisliuk A, Pipes RB, Pyrz R, Sokolov AP. Microscopic mechanism of reinforcement in single-wall carbon nanotube/polypropylene nanocomposite. Polymer 2005; 46: 439–44.

[2] Thostenson ET, Ren Z, Chou T. Advances in the science and technology of carbon nanotubes and their composites: a review. Composites Science and Technology 2001; 61: 1899–912.

[3] Nogales A, Broza G, Roslaniec Z, Schulte K, Sics I, Hsiao BS, Sanz A, Garcia-Gutierrez MC, Rueda DR, Domingo C, Ezquerra TA. Low percolation threshold in nanocomposites based on oxidized single wall carbon nanotubes and poly(butylene terephthalate). Macromolecules 2004; 37: 7669–72.

[4] Krause B, Pötschke P, Häussler L. Influence of small scale melt mixing conditions on electrical resistivity of carbon nanotube-polyamide composites. Composites Science and Technology 2009; 69: 1505–15.

[5] Bauhofer W, Kovacs JZ. A review and analysis of electrical percolation in carbon nanotube polymer composites. Composites Science and Technology 2009; 69: 1486–98.

[6] Spitalsky Z, Tasis D, Papagelis K, Galiotis C. Carbon nanotube-polymer composites: Chemistry, processing, mechanical and electrical properties. Progress in Polymer Science; In Press, Corrected Proof.

[7] Yu S, Wong WM, Hu X, Juay YK. The characteristics of carbon nanotube-reinforced poly(phenylene sulfide) nanocomposites. Journal of Applied Polymer Science 2009; 113: 3477–83.

[8] Grossiord N, Loos J, Regev O, Koning CE. Toolbox for Dispersing Carbon Nanotubes into Polymers To Get Conductive Nanocomposites. Chemistry of Materials 2006; 18: 1089–99.

[9] Breuer O, Sundararaj U. Big returns from small fibers: A review of polymer/carbon nanotube composites. Polymer Composites 2004; 25: 630–45.

[10] Pegel S, Pötschke P, Petzold G, Alig I, Dudkin SM, Lellinger D. Dispersion, agglomeration, and network formation of multiwalled carbon nanotubes in polycarbonate melts. Polymer 2008; 49: 974–84.

[11] Ajayan PM, Tour JM. Materials science - Nanotube composites. Nature 2007; 447: 1066–68.

[12] Villmow T, Pötschke P, Pegel S, Häussler L, Kretzschmar B. Influence of twin-screw extrusion conditions on the dispersion of multi-walled carbon nanotubes in a poly(lactic acid) matrix. Polymer 2008; 49: 3500–09.

[13] Micusik M, Omastova M, Krupa I, Prokes J, Pissis P, Logakis E, Pandis C, Pötschke P, Pionteck J. A comparative study on the electrical and mechanical behaviour of multi-walled carbon nanotube composites prepared by diluting a masterbatch with various types of polypropylenes. J. Appl. Polym. Sci. 2009; 113: 2536–51.

[14] Kasaliwal GR, Pegel S, Göddel A, Pötschke P, Heinrich G. Analysis of agglomerate dispersion mechanisms of multiwalled carbon nanotubes during melt mixing in polycarbonate. Polymer 2010; 51: 2708–20.

[15] Kasaliwal G, Gödel A, Pötschke P. Influence of processing conditions in small-scale melt mixing and compression molding on the resistivity and morphology of polycarbonate-MWNT composites. Journal of Applied Polymer Science 2009; 112: 3494–509.

[16] Villmow T, Kretzschmar B, Pötschke P. Influence of screw configuration, residence time, and specific mechanical energy in twin-screw extrusion of polycaprolactone/multi-walled carbon nanotube composites. Composites Science and Technology 2010; 70: 2045–55.

[17] Chang L, Friedrich K, Ye L, Toro P. Evaluation and visualization of the percolating networks in multi-wall carbon nanotube/epoxy composites. Journal of Materials Science 2009; 44: 4003–12.

[18] Loos J, Grossiord N, Koning CE, Regev O. On the fate of carbon nanotubes: Morphological characterisations. Composites Science and Technology 2007; 67: 783–88.

[19] Deng H, Zhang R, Bilotti E, Loos J, Peijs T. Conductive polymer tape containing highly oriented carbon nanofillers. Journal of Applied Polymer Science 2009; 113: 742–51.

[20] Hill HW, Brady DG. Properties, environmental stability, and molding characteristics of polyphenylene sulfide. Polymer Engineering & Science 1976; 16: 831–35.

[21] Cheng SZD, Wu ZQ, Wunderlich B. Glass-transition and Melting Behavior of Poly(thio-1,4-phenylene). Macromolecules 1987/november; 20: 2802–10.

[22] Yang J, Xu T, Lu A, Zhang Q, Tan H, Fu Q. Preparation and properties of poly (p-phenylene sulfide)/multiwall carbon nanotube composites obtained by melt compounding. Composites Science and Technology 2009; 69: 147–53.

[23] Wu D, Wu L, Gao F, Zhang M, Yan C, Zhou W. Poly(phenylene sulfide) magnetic composites. I. Relations of percolation between rheology, electrical, and magnetic properties. Journal of Polymer Science Part B: Polymer Physics 2008; 46: 233–43.

[24] Han MS, Lee YK, Lee HS, Yun CH, Kim WN. Electrical, morphological and rheological properties of carbon nanotube composites with polyethylene and poly(phenylene sulfide) by melt mixing. Chemical Engineering Science 2009; 64: 4649–56.

[25] Stauffer D, Aharony A. Introduction to percolation theory. London: Taylor & Francis; 1992.

[26] Tessonnier J, Rosenthal D, Hansen TW, Hess C, Schuster ME, Blume R, Girgsdies F, Pfänder N, Timpe O, Su DS, Schloegl R. Analysis of the structure and chemical properties of some commercial carbon nanostructures. Carbon 2009; 47: 1779–98.
[27] Knör N. Einfluss der Verarbeitungstechnologie und Werkstoffzusammensetzung auf die Struktur Eigenschaftsbeziehungen von thermoplastischen Nanoverbundwerkstoffen. IVW Schriftenreihe; Hrsg. Prof. Dr.-Ing. Peter Mitschang; Bd. 92 2010; ISBN 978-3-930-89-6.
[28] Lellinger D, Xu DH, Ohneiser A, Skipa T, Alig I. Influence of the injection moulding conditions on the in-line measured electrical conductivity of polymer-carbon nanotube composites. Physica Status Solidi B-basic Solid State Physics 2008; 245: 2268–71.
[29] Villmow T, Pegel S, Pötschke P, Wagenknecht U. Influence of injection molding parameters on the electrical resistivity of polycarbonate filled with multi-walled carbon nanotubes. Composites Science and Technology 2008; 68: 777–89.
[30] Chung KT, Reisner JH, Campbell ER. Charging Phenomena In the Scanning Electron-microscopy of Conductor-insulator Composites - A Tool For Composite Structural-analysis. Journal of Applied Physics 1983; 54: 6099–112.
[31] Battisti A, Skordos AA, Partridge IK. Monitoring dispersion of carbon nanotubes in a thermosetting polyester resin. Composites Science and Technology 2009; 69: 1516–20.
[32] Broadbent S, Hammersley J. Percolation processes I. Crystals and mazes. Proceedings of the Cambridge Philosophical Society 1957; 53: 629–41.
[33] Lux F. Models Proposed To Explain the Electrical-conductivity of Mixtures Made of Conductive and Insulating Materials. Journal of Materials Science 1993; 28: 285–301.
[34] Kirkpatrick S. Percolation and Conduction. Rev. Mod. Phys. 1973; 45: 574–88.
[35] Weber M, Kamal MR. Estimation of the volume resistivity of electrically conductive composites. Polymer Composites 1997; 18: 711–25.
[36] Lisunova MO, Mamunya YP, Lebovka NI, Melezhyk AV. Percolation behaviour of ultrahigh molecular weight polyethylene/multi-walled carbon nanotubes composites. European Polymer Journal 2007; 43: 949–58.
[37] Logakis E, Pollatos E, Pandis C, Peoglos V, Zuburtikudis I, Delides CG, Vatalis A, Gjoka M, Syskakis E, Viras K, Pissis P. Structure-property relationships in isotactic polypropylene/multi-walled carbon nanotubes nanocomposites. Composites Science and Technology 2010; 70: 328–35.
[38] Bhattacharya S, Tandon R, Sachdev V. Electrical conduction of graphite filled high density polyethylene composites; experiment and theory. Journal of Materials Science 2009; 44: 2430–33.
[39] Shaffer MSP, Windle AH. Fabrication and Characterization of Carbon Nanotube/Poly(vinyl alcohol) Composites. Advanced Materials 1999; 11: 937–41.
[40] Foygel M, Morris RD, Anez D, French S, Sobolev VL. Theoretical and computational studies of carbon nanotube composites and suspensions: Electrical and thermal conductivity. Phys. Rev. B 2005; 71.
[41] Bauhofer W, Schulz SC, Eken AE, Skipa T, Lellinger D, Alig I, Tozzi EJ, Klingenberg DJ. Shear-controlled electrical conductivity of carbon nanotubes networks suspended in low and high molecular weight liquids. Polymer 2010; 51: 5024–27.
[42] Alig I, Skipa T, Lellinger D, Bierdel M, Meyer H. Dynamic percolation of carbon nanotube agglomerates in a polymer matrix: comparison of different model approaches. phys. stat. sol. (b) 2008; 245: 2264–67.
[43] Kovacs JZ, Velagala BS, Schulte K, Bauhofer W. Two percolation thresholds in carbon nanotube epoxy composites. Composites Science and Technology 2007; 67: 922–28.
[44] Pegel S, Pötschke P, Villmow T, Stoyan D, Heinrich G. Spatial statistics of carbon nanotube polymer composites. Polymer 2009; 50: 2123–32.
[45] Logakis E, Pandis C, Kyritsis A, Pissis P, Micusi-k M, Omastova M, Pionteck J. Indirect methods for the determination of optimal processing conditions in conductive polypropylene/carbon nanotubes composites. Chemical Physics Letters 2010; 498: 125–28.
[46] Skipa T, Lellinger D, Böhm W, Saphiannikova M, Alig I. Influence of shear deformation on carbon nanotube networks in polycarbonate melts: Interplay between build-up and destruction of agglomerates. Polymer 2010; 51: 201–10.

Figure 1

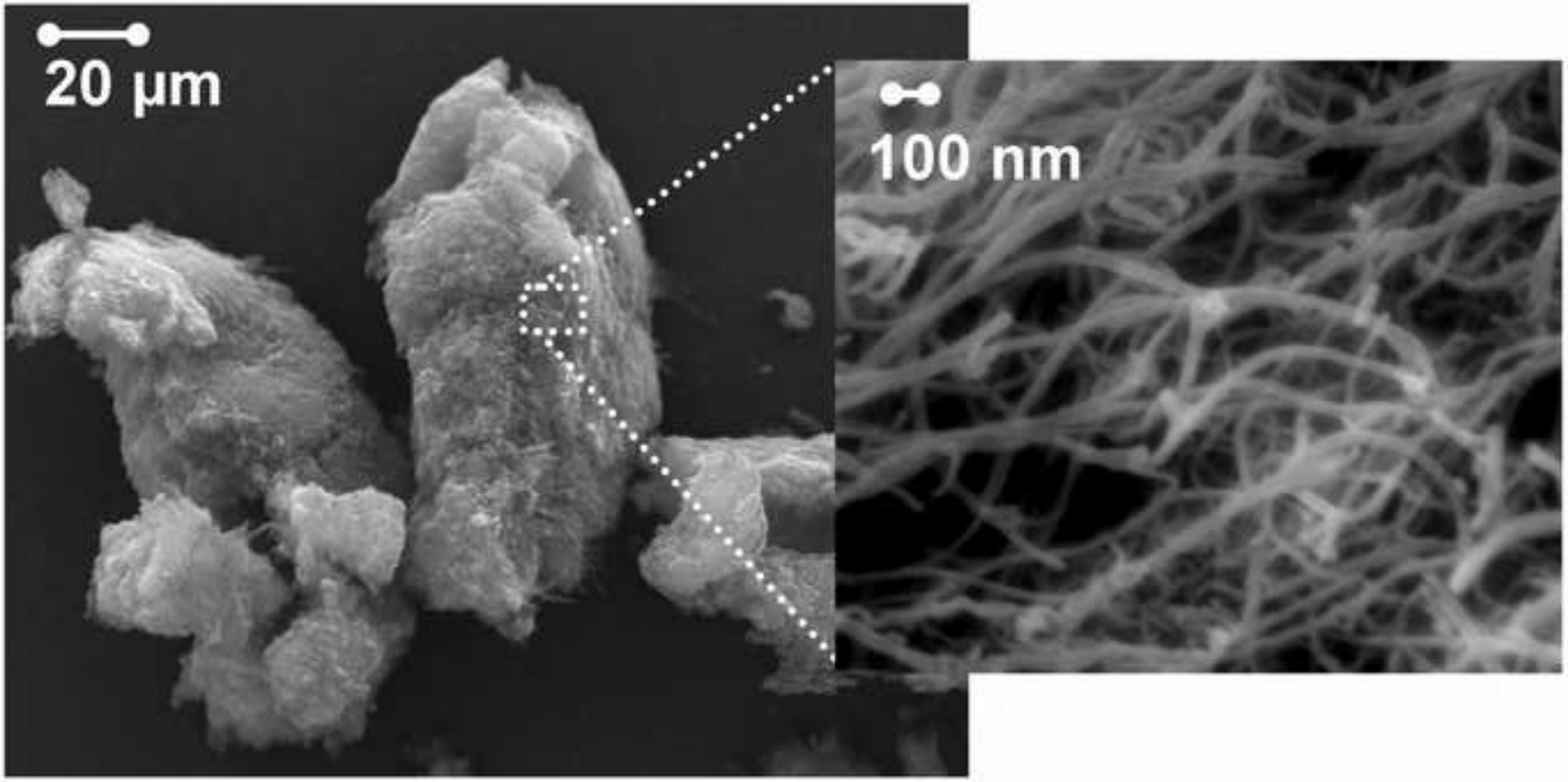

Figure 2

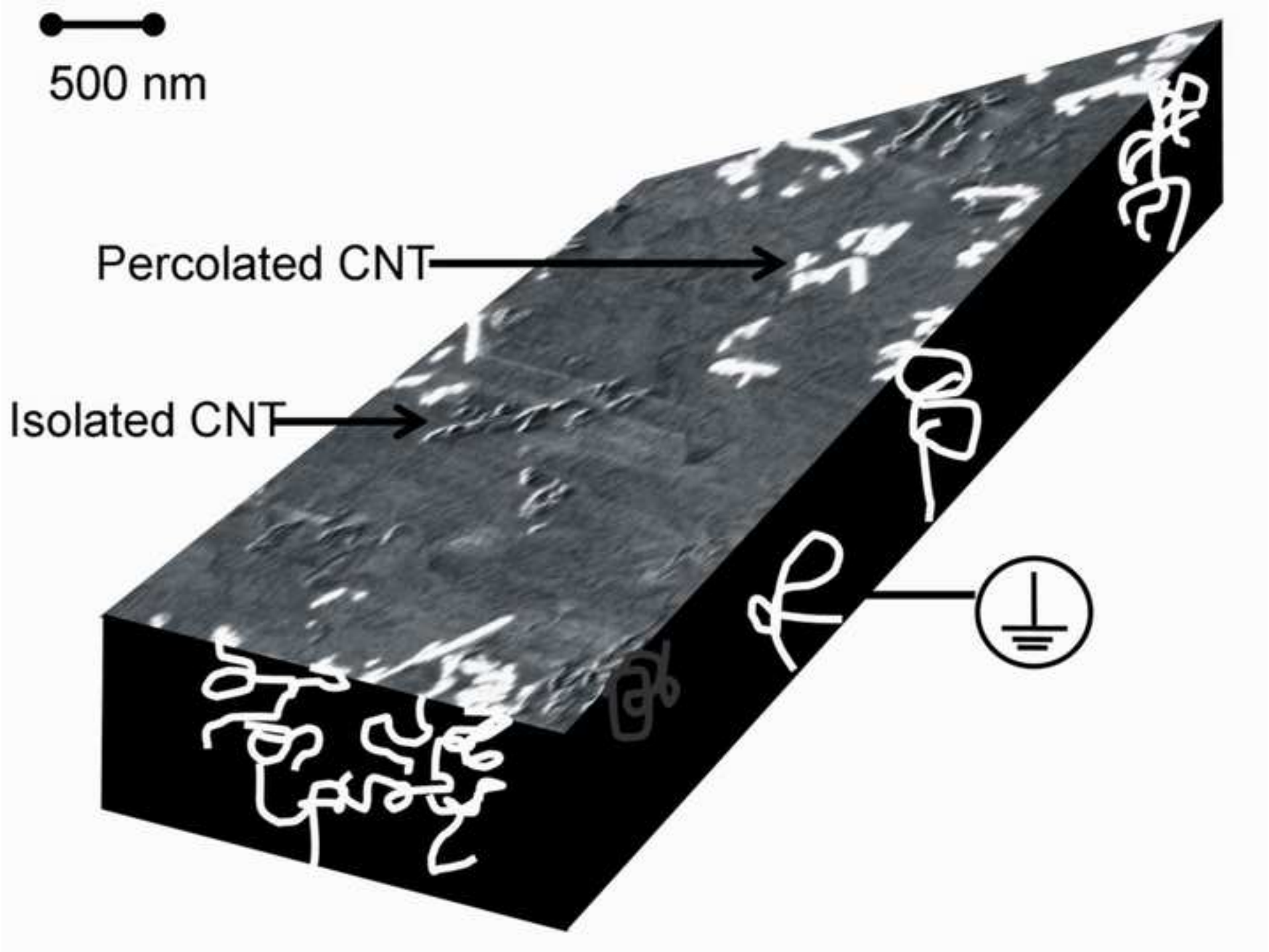

Figure 3

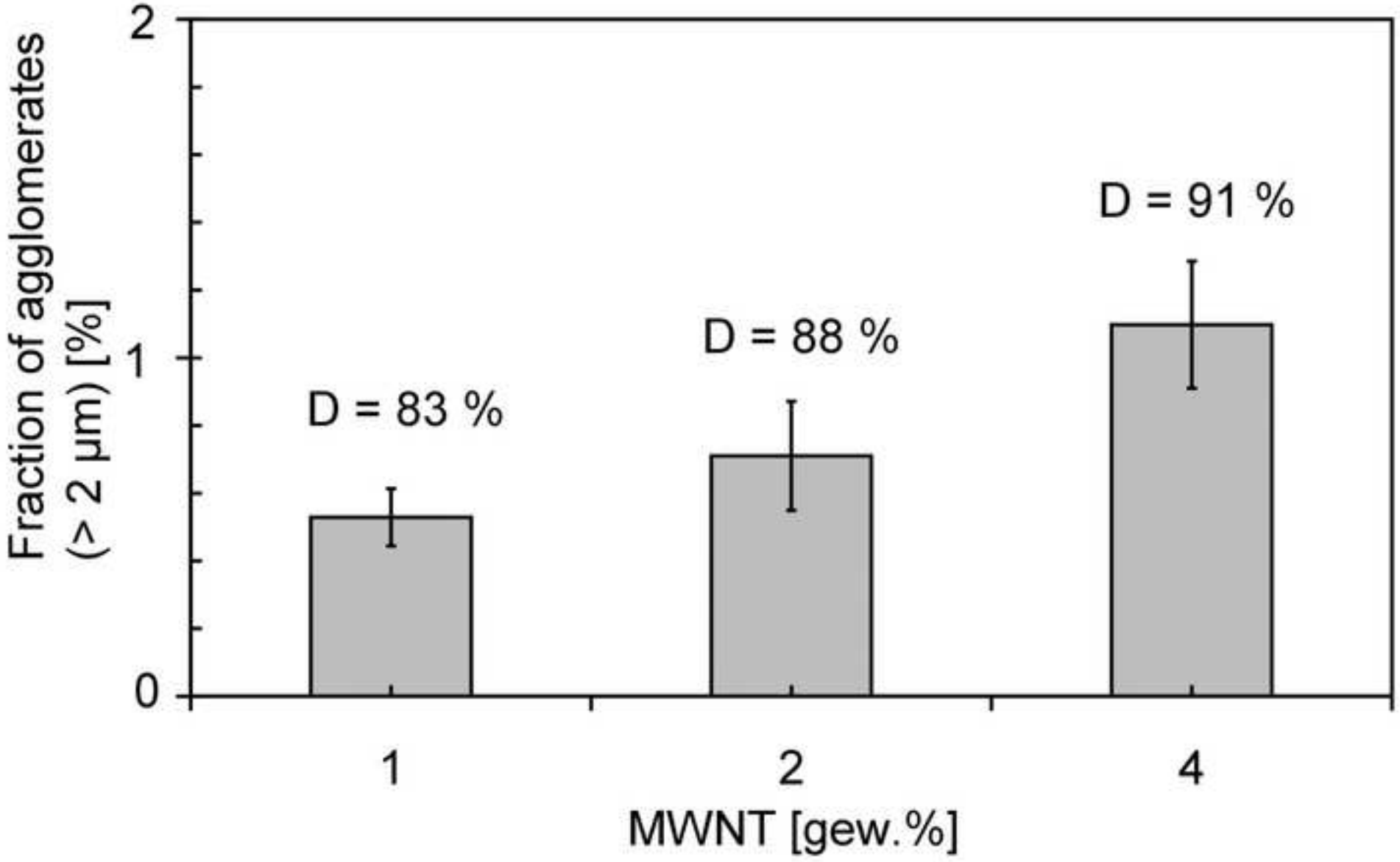

Figure 4

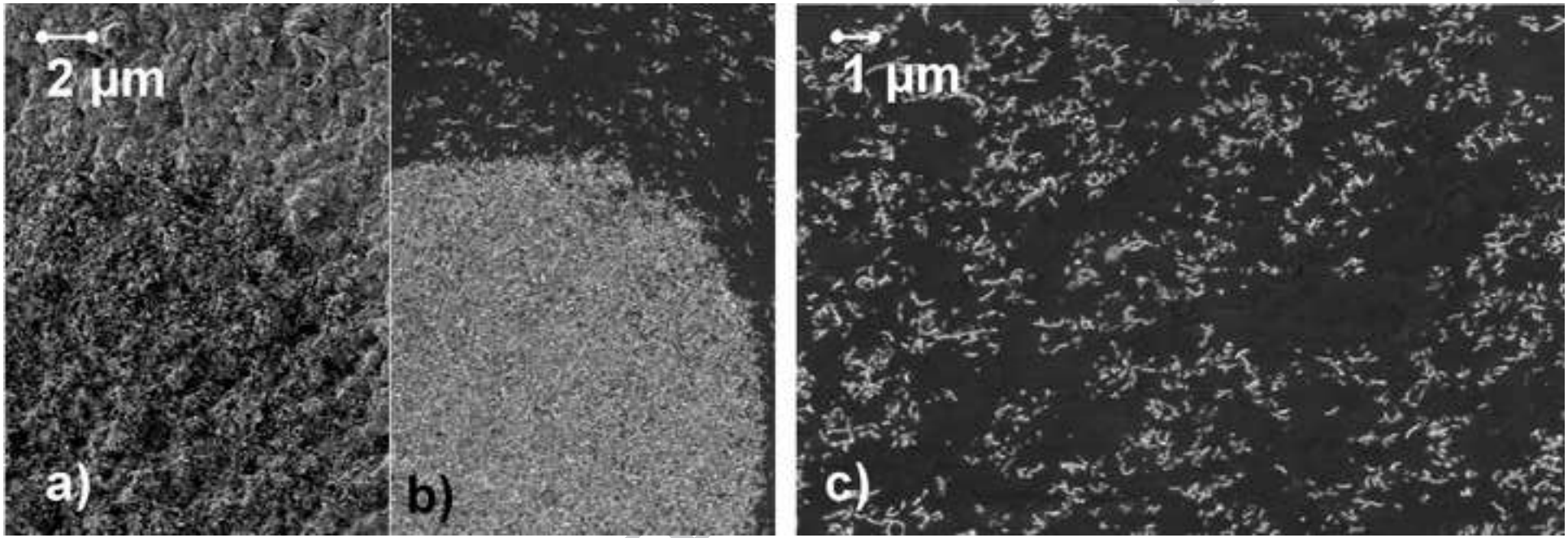

Figure 5

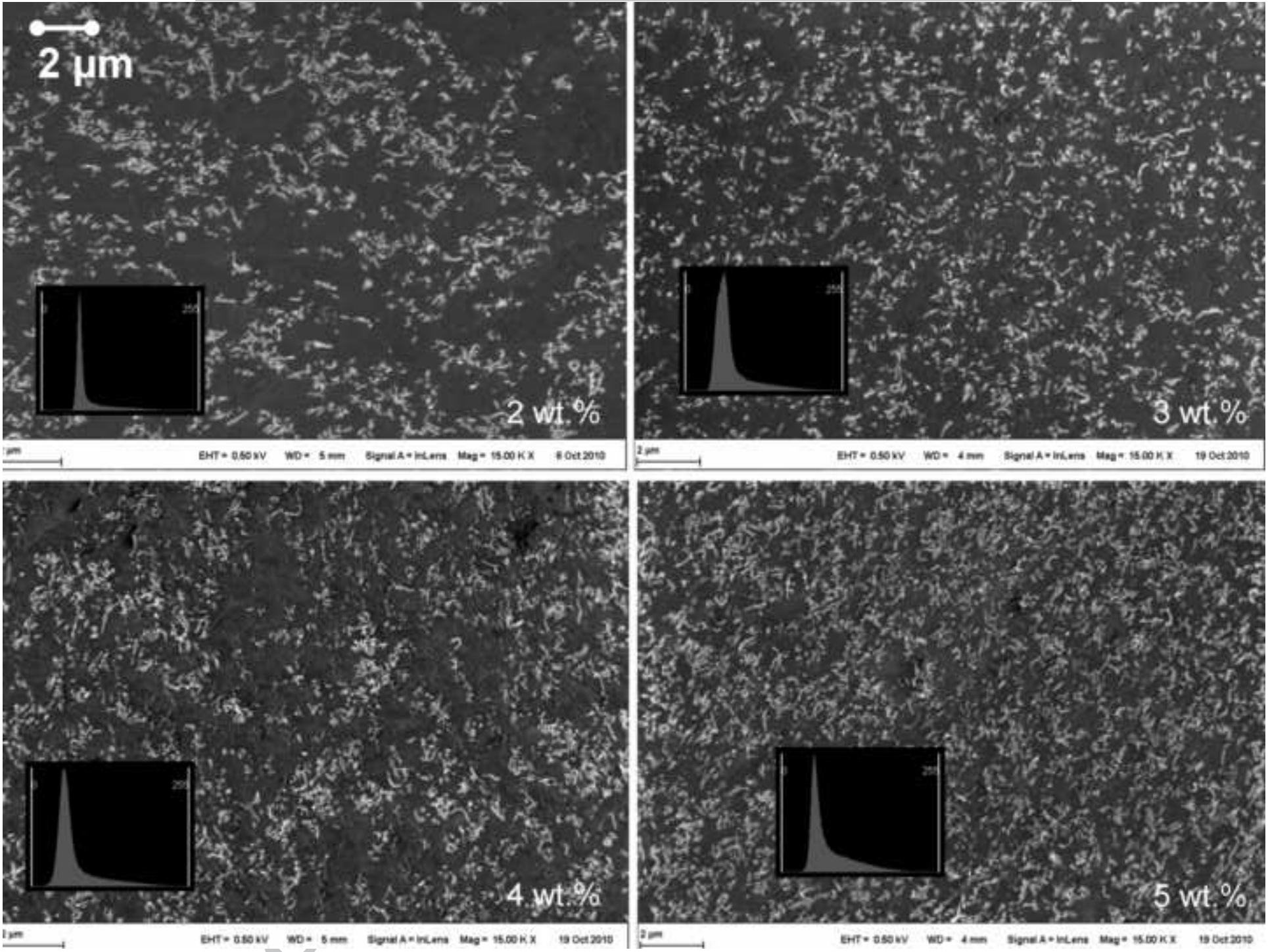

Figure 6

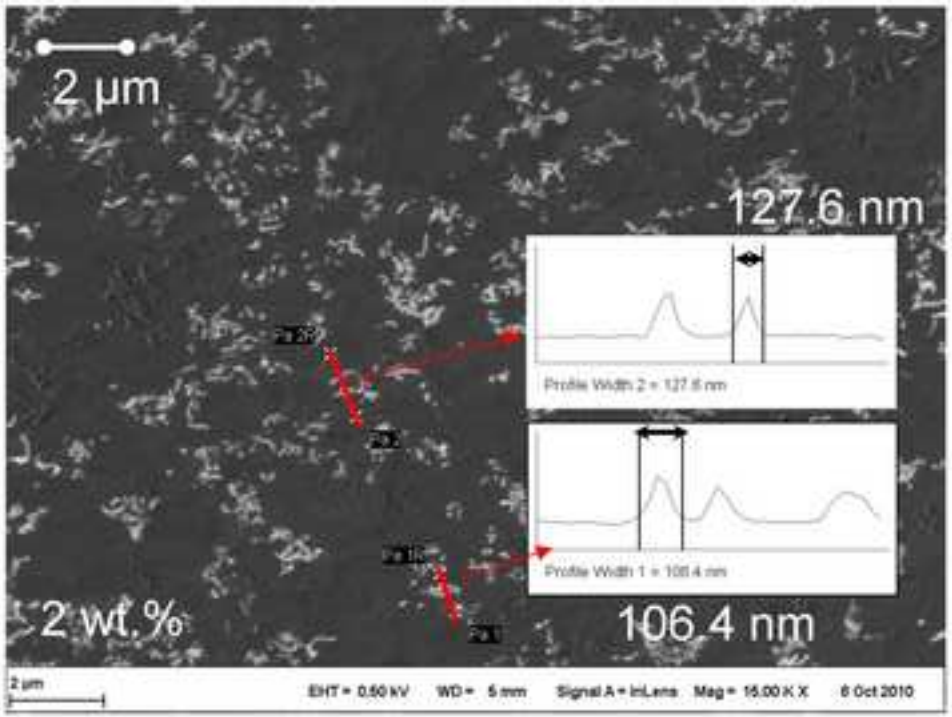

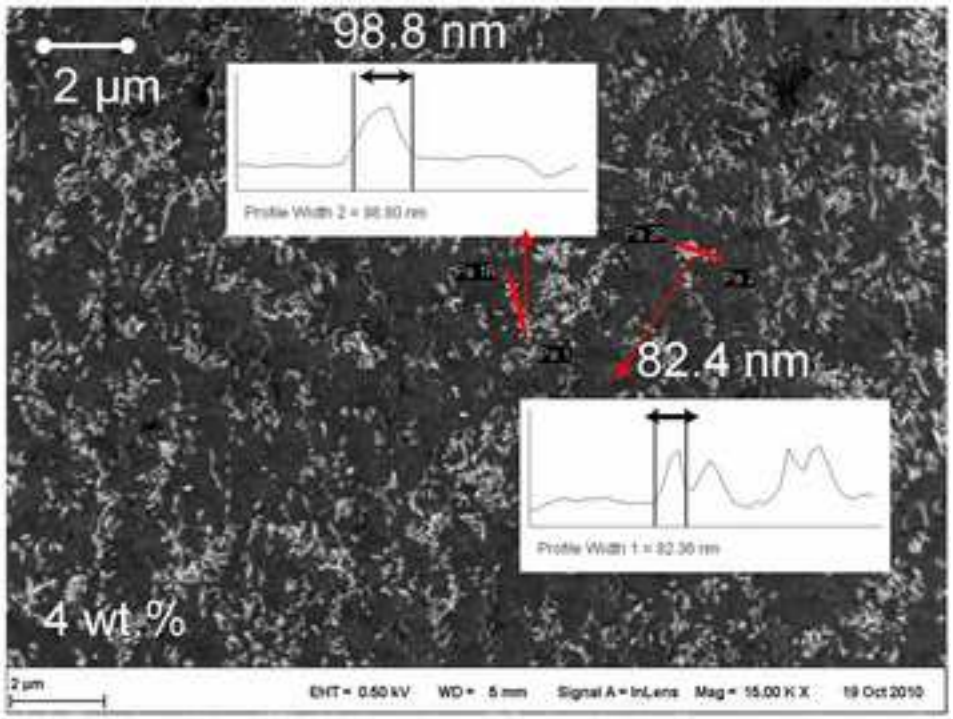

Figure 7

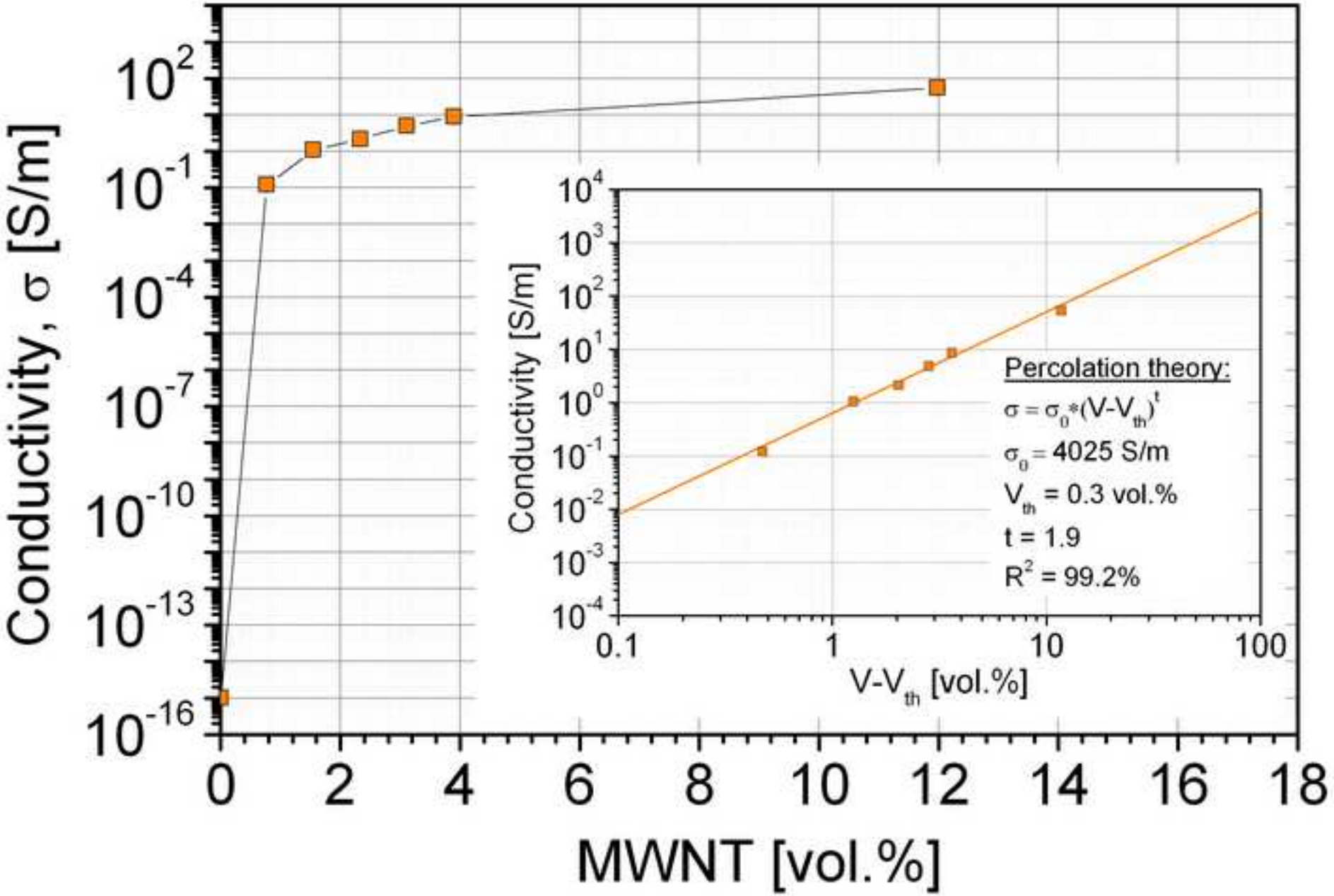

Figure 8